BIO Integration

Morphological Evaluation of Mitral Valve Based on Three-dimensional Printing Models: Potential Implication for Mitral Valve Repair

Yuanting Yang[1,a], Hao Wang[1,a], Hongning Song[1], Yugang Hu[1], Qincheng Gong[1], Ye Xiong[1], Junbi Liu[1], Wei Ren[2] and Qing Zhou[1,*]

Abstract

Objective: This study aimed to analyze the morphological characteristics of rheumatic (RMVD) and degenerative mitral valve diseases (DMVD) based on three-dimensional (3D) printing model before and after surgery and to explore the potential implication of the 3D printing model for mitral valve (MV) repair.
Methods: 3D transesophageal echocardiography (TEE) data of the MV were acquired in 45 subjects (15 with RMVD, 15 with DMVD, and 15 with normal MV anatomy). 3D printing models of the MV were constructed by creating molds to be printed with water-soluble polyvinyl alcohol, then filled with room temperature vulcanizing silicone. The parameters of the annulus and leaflet of the MV were acquired and analyzed using the 3D printing model. Mitral valve repair was simulated on 3D printing models of 10 subjects and compared with the actual operation performed on patients. The effects of surgery were assessed by evaluating the changes in coaptation length (CL) and the annular height to commissural width ratio (AHCWR) before and after MV repairs. The correlations of the grade of mitral regurgitation with CL and AHCWR were analyzed.
Results: 3D silicone MV models were all successfully constructed based on 3D TEE data. Compared with the normal groups, the mitral annulus size in the RMVD groups showed no significant differences. In contrast, mitral annulus in DMVD groups was dilated and flattened with diameters of anteroposterior, anterolateral-posteromedial, commissural width, annular circumferences, and area increased. Mitral repair was successfully simulated on 10 models with significant increase in leaflet coaptation area both in vivo and in vitro. Good agreement was observed in CL and AHCWR after surgery in the 3D printing model compared with real surgery on the patient valve. The grade of mitral regurgitation correlated inversely with CL ($r = -0.87$, $P < 0.01$) and AHCWR ($r = -0.79$, $P < 0.01$). Mitral valve repair was performed twice in one model to assess which provided a better outcome.
Conclusions: 3D printing models of the MV based on 3D TEE data could be used in morphological analysis of the MV before and after surgery in RMVD and DMVD. Surgery simulation on 3D printing models could provide valuable information concerning morphological changes after surgery, with are closely associated with clinical outcomes.

Keywords

Mitral repair, surgical simulation, three-dimensional, 3D printing, transesophageal echocardiography.

[1]Department of Ultrasound Imaging, Renmin Hospital of Wuhan University, Wuhan 430060, China

[2]Department of Cardiovascular Surgery, Renmin Hospital of Wuhan University, Wuhan 430060, China

[a]These authors contributed equally to this work.
*Correspondence to: Qing Zhou, E-mail: qingzhou.wh.edu@hotmail.com

Received: July 22 2021
Revised: October 18 2021
Accepted: November 3 2021
Published Online: November 30 2021

Available at: https://bio-integration.org/

Background

Mitral valve (MV) disease is the most common type of valvular disease [1]. Rheumatic and degenerative diseases are common causes of primary MV disease [2]. Morphology assessment of the MV provides an insight into the etiology and severity of valve disease, which is essential for surgical and interventional treatment [3].

Compared with computer tomography (CT), echocardiography can dynamically display the movement of the valve in real-time, and has a higher resolution of the valve. It has become the crucial technique for diagnosing and evaluating the degree of valve disease [4]. Two-dimensional (2D) echocardiography can display the valve through sectional images, which is not conducive to surgeons' understanding. Three-dimensional (3D) echocardiography technology can reconstruct a 3D virtual valve in just a few minutes, providing a surgical perspective of the MV anatomy. However, both 2D and 3D images on a two-dimensional screen, not a physical model, have limitations in surgical applications [5]. However, 3D printing models, which intuitively display the pathology

structure of the annulus and leaflets, could act as a bridge between 2D images and clinical doctors. It can provide the surgeon with a physical model for simulation operation, which is not available in 2D images.

Accordingly, the objectives of our study are twofold: to describe the morphological characteristics of rheumatic and degenerative MV diseases based on 3D printing models and to explore the potential role of 3D printing models on surgical planning and evaluation of MV repair.

Materials and methods

Study population

This study enrolled 30 patients with mitral valvular disease who had pre-procedure transesophageal echocardiography (TEE) at the People's Hospital of Wuhan University from January 2018 to August 2019 consisting of 12 males and 18 females, aged 32 to 71 years (mean, 57.75 ± 11.10 years). Fifteen cases had rheumatic mitral valve disease (RMVD) and 15 cases had degenerative mitral valve disease (DMVD, including 10 cases of MV prolapse). In addition, a control group of 15 age-matched patients with normal MV anatomy was also studied. Patients with contraindications to TEE and those with any type of cardiac arrhythmia, myocarditis, pericardial, or congenital heart disease were excluded from this study. All patients were in sinus rhythm. The Ethics Committee approved the study protocols at the People's Hospital of Wuhan University.

3D printing of the silicone MV model

The 3D TEE data were obtained by GE Vivid E9 equipped with a 3- to 8-MHz transesophageal matrix-array transducer. All patients were monitored by synchronized electrocardiogram, and the 3D TEE probe was placed in the middle esophagus to acquire full-volume 3D images. Five consecutive cardiac cycles of the full-volume data set with good quality and clarity were stored and explored to an EchoPac workstation.

The original data in the Digital Imaging and Communications in Medicine format were exported into medical image segmentation software (Materialise Mimics version 19.0; Materialise, Leuven, Belgium). The selected diastolic and systolic images were manually segmented using threshold settings to create a region of interest containing the MV. Subsequently, crop mask was determined by adjusting the sampling frame to include the MV. Trimming and drawing tools were employed to reduce the noise of blood and manually manipulate the shape of the anterior and posterior leaflets. 3D digital models of the MV were then calculated automatically using the calculating 3D function.

Then, the 3D digital models were exported to computer-aided design software (Materialise 3-Matic; Materialise) and refined by the local smoothing tools. Based on the 3D digital models, the boolean subtraction function was utilized to render a mold by offsetting the original MV model by 2 mm. A pipe was added to connect the cavity of the mold for pouring silicone. The 3D mold of the MV models was exported in stereolithography format (.stl) for 3D printing.

The STL file was later transformed to the 3D JG AURORA printer (Shenzhen Aurora Technology Co., Ltd., Shenzhen, China), in which the 3D mold was printed using water-soluble polyvinyl alcohol (ESUN PVA 1.75 mm; ESUN New Materials Co., Ltd., Hubei, China). Then the mold was filled with room temperature vulcanizing (RTV) silicone rubber (Hong Cheng Silicone Products Factory, Guangdong, China) using a syringe. The silicone MV model was removed from the mold once the PVA mold dissolved substantially (**Figure 1**).

Quantitative assessment of mitral morphology

From 3D printing MV model, several parameters were calculated: annular geometry characteristics, including the anteroposterior (AP) diameter, anterolateral-posteromedial (AL-PM) diameter, commissural width (CW), and annular height (AH), were measured with a vernier caliper. Annular circumference (AC) and area (A) were measured by soft aluminum wire shaping, and the AHCWR was defined as the ratio of annular height to commissural width [6]; leaflet size: the length of the anterior (AL) and posterior (PL) leaflets were measured with a vernier caliper. Soft aluminum wire shaping measured the anterior (AA) and posterior (PA) leaflet areas. The data were analyzed 2 days apart by the same observers (intraobserver) and a different observer (interobserver) blinded to the initial results, and the average value was used for statistical analysis.

Simulated mitral repair on 3D printing model

The MV models of 10 patients with the degenerative disease who intend to undergo MV repairs were set up on a benchtop to simulate operation (**Figure 2**). Two experienced surgeons were invited to simulate the procedure using our 3D MV model. The mitral repair techniques employed included leaflet resection and ring annuloplasty. Assessments for mitral repair included the coaptation length (CL) and AHCWR in the model valves, and CL was measured as the mean coaptation length of the region where the anterior and posterior leaflets overlap (**Figure 3**). According to previous studies [7, 8], a strong inverse correlation existed between AHCWR and mitral regurgitation. The mitral regurgitation grades before and after the actual repair were recorded.

Statistical analysis

Statistical analysis was performed using SPSS version 21.0 software (2012 release; IBM Corp., Armonk, NY, USA) and Medcalc version 11.0 (Medcalc Software, MedCalc

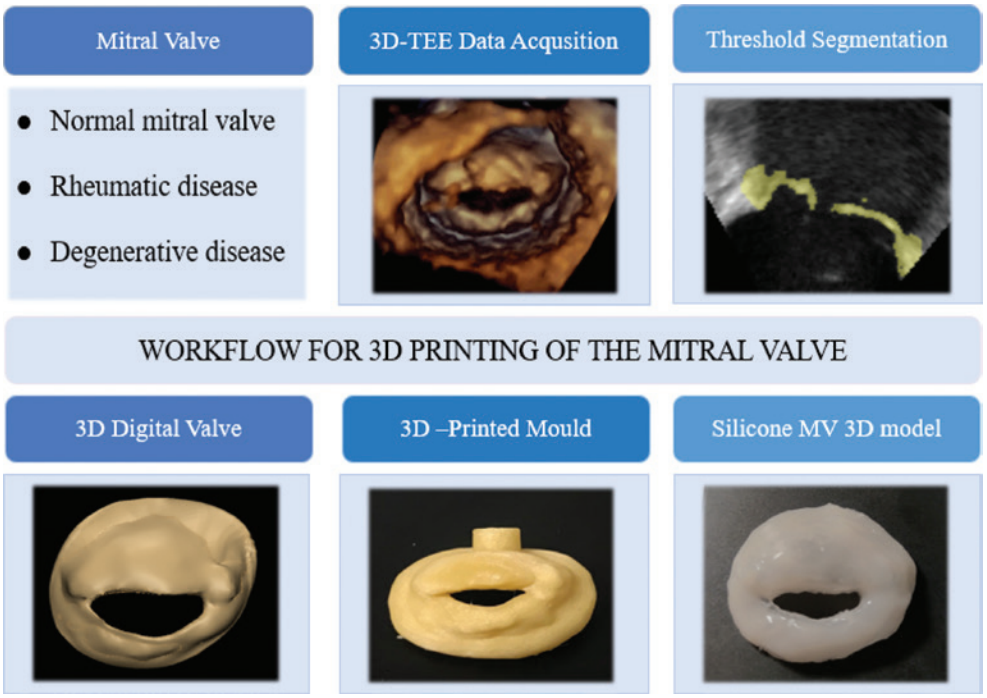

Figure 1 Workflow associated with printing a three-dimensional (3D) silicone model of the mitral valve. A sample of the workflow is shown from the transesophageal acquisition of the 3D echocardiography data set to its segmentation and creation of a virtual 3D model and mold that can be printed using water-soluble polyvinyl alcohol. The 3D model of the valve can be used to appreciate valve morphology and perform qualitative and quantitative analysis useful for pre-procedural planning.

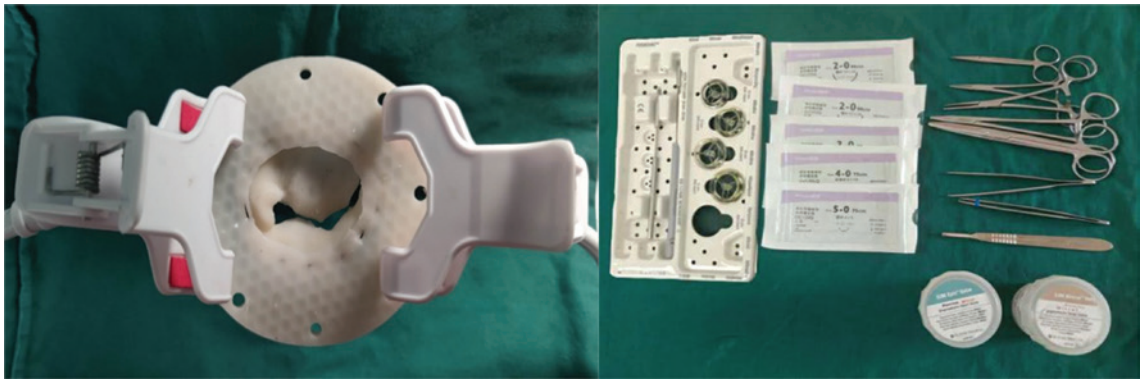

Figure 2 Surgical setup. The silicone mitral valve model was braced by clamps over the operative table for simulation operation.

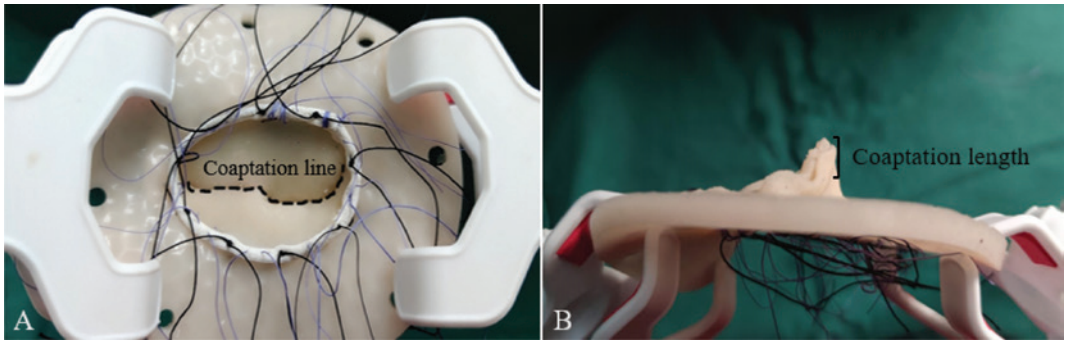

Figure 3 Measurement of the coaptation length. (A) Coaptation line (black dotted line). (B) Coaptation length. This was measured as the mean coaptation length of the region where the anterior and posterior leaflets overlap.

Software Ltd., Ostend, Belgium). Continuous variables were presented as means ± standard deviations, and categorical variables were presented as frequencies or percentages. The intraclass correlation coefficient was used to assess the intraobserver and interobserver variabilities of the 3D printing model morphology measurements. The agreement of CL and AHCWR between the simulated operation and the actual surgery was presented as Bland-Altman plots. Spearman's

correlation analysis and partial correlation analysis were applied to analyze the relationship between mitral regurgitation grades with CL and AHCWR. $P < 0.05$ was considered statistically significant.

Results

The baseline clinical and echocardiographic characteristics of the patients (15 with RMVD, 15 with DMVD, and 15 controls) are presented in **Table 1**. Patients with RMVD and DMVD had a higher New York Heart Association classification than the control group. The left ventricular volumes of the DMVD group were greater that those of the RMVD and control groups, but the ejection fraction of the DMVD group was similar to that of the RMVD and control groups.

The 3D TEE data of all 45 patients were post-processed, and the 3D models were printed out at a 1:1 ratio. Printing time depends on the complexity of the valve anatomy. The 3D reconstruction of digital model was approximately 60 to 85 minutes for each case. Post-processing procedures required 20 to 30 minutes. The mold printing was approximately 3 to 4 hours. Pouring RTV and dissolving mold required 2 to 3 hours.

Morphological analysis on the MV model

Compared with 3D TEE images, the morphological parameters measured on our 3D printing model showed great consistency. No significant differences were found (**Table 2**). The absolute difference between the 3D printing model and the 3D TEE image indicated that the model's accuracy was within 2 mm (**Table 3**). Such results demonstrated that the mold-molding method might be used to produce the patient-specific MV models with high accuracy. The interobserver and intraobserver intraclass correlation coefficients of the measurements of MV morphology were good (**Table 4**).

Table 1 Clinical and Echocardiographic Characteristics in Controls and Patients with RMVD and DMVD

Variable	Controls (n = 15)	RMVD (n = 15)	*P*	DMVD (n = 15)	*P*
Clinical					
Age (years)	56.7 ± 11.1	58.6 ± 10.9	0.231	60.7 ± 13.1	0.068
Men	8 (53)	7 (47)	0.278	9 (60)	0.198
BSA (m^2)	1.8 ± 0.2	1.9 ± 0.5	0.089	1.8 ± 0.9	0.102
NYHA class			<0.001		<0.001
I	15 (100)	5 (33)		4 (27)	
II	0 (0)	10 (67)		11 (73)	
III/IV	0 (0)	0 (0)		0 (0)	
Echocardiographic					
LVEDV (mL/m^2)	54 ± 8	68 ± 10	<0.001	72 ± 8	<0.001
LVESV (mL/m^2)	21 ± 6	25 ± 9	<0.001	28 ± 10	<0.001
LVEF (%)	61 ± 10	63 ± 14	0.372	62 ± 16	0.110

Data are expressed as mean ± standard deviation or number (percentage).
BSA, body surface area; DMVD, degenerative mitral valve disease; LVEDV, left ventricular end-diastolic volume; LVEF, left ventricular ejection fraction; LVESV, left ventricular end-systolic volume; NYHA, New York Heart Association; RMVD, rheumatic mitral valve disease.

Table 2 Comparison of Measurements Performed on the 3D Printing Model of the MV and on the 3D TEE Image

Groups	AP (cm)	AL-PM (cm)	AC (cm)	A (cm^2)	AL (cm)	PL (cm)
Controls (n = 15)						
3D printing model	2.89 ± 0.30	3.29 ± 0.31	10.66 ± 0.82	8.05 ± 1.60	2.21 ± 0.37	1.21 ± 0.30
3D TEE	2.97 ± 0.21	3.31 ± 0.54	10.71 ± 0.43	8.01 ± 1.45	2.11 ± 0.28	1.10 ± 0.24
t	0.04	0.22	0.06	0.46	0.62	0.78
P	0.94	0.81	0.95	0.64	0.55	0.46
RMVD (n = 15)						
3D printing model	3.34 ± 0.43	3.45 ± 0.60	11.10 ± 0.80	10.30 ± 1.30	2.66 ± 0.28	1.44 ± 0.23
3D TEE	3.41 ± 0.24	3.52 ± 0.64	11.21 ± 0.86	10.53 ± 1.33	2.72 ± 0.38	1.33 ± 0.43
t	0.01	0.05	0.02	0.13	0.38	–0.94
P	0.96	0.95	0.98	0.88	0.72	0.37
DMVD (n = 15)						
3D printing model	3.52 ± 0.71	3.98 ± 0.34	12.15 ± 1.61	11.72 ± 1.10	2.38 ± 0.45	1.42 ± 0.43
3D EE	3.64 ± 0.81	3.82 ± 0.42	12.23 ± 0.91	11.84 ± 0.43	2.25 ± 0.55	1.31 ± 0.62
t	0.06	0.05	0.01	0.03	–0.85	–0.93
P	0.94	0.95	0.99	0.97	0.42	0.38

3D, three-dimensional; AP, antero-posterior diameters; AL-PM, anterolateral and posteromedial diameters; AC, annular circumferences; A, annular area; AL, length of anterior leaflet; PL, length of posterior leaflet; TEE, transesophageal echocardiography.

Table 3 Comparison of Absolute Difference between the 3D Printing Model and 3D the Transesophageal Echocardiography Parameters

Groups	AP (cm)	AL-PM (cm)	AC (cm)	A (cm^2)	AL (cm)	PL (cm)
Controls	0.09 ± 0.07	0.06 ± 0.02	0.07 ± 0.04	0.08 ± 0.05	0.07 ± 0.05	0.09 ± 0.05
RMVD	0.05 ± 0.01	0.09 ± 0.06	0.12 ± 0.06	0.13 ± 0.06	0.05 ± 0.04	0.13 ± 0.04
DMVD	0.12 ± 0.03	0.16 ± 0.04	0.10 ± 0.05	0.11 ± 0.05	0.15 ± 0.03	0.12 ± 0.08

3D, three-dimensional; A, annular area; AC, annular circumferences; AL, length of anterior leaflet; AL-PM, anterolateral and posteromedial diameters; AP, anteroposterior diameters; DMVD, degenerative mitral valve disease; PL, length of posterior leaflet; RMVD, rheumatic mitral valve disease; TEE, transesophageal echocardiography.

Table 4 Strength of Agreement of the Interobserver and Intraobserver Analyses for Each Mitral Valve Parameter Measured on Three-dimensional Printing Model

Parameters	Intraclass Correlation Coefficients	
	Intraobserver	Interobserver
AP	0.842	0.812
AL-PM	0.902	0.897
CW	0.817	0.810
AC	0.942	0.932
A	0.923	0.897
AH	0.934	0.923
AHCWR	0.916	0.903
AL	0.926	0.917
PL	0.893	0.867
AA	0.876	0.865
PA	0.925	0.915

A, annular area; AA, anterior leaflet area; AC, annular circumference; AH, annular height; AHCWR, annular height to commissural width ratio; AL, length of anterior leaflet; AL-PM, anterolateral and posteromedial diameters; AP, anteroposterior diameters; CW, commissural width; PA, area of posterior leaflet; PL, length of posterior leaflet.

Table 5 Measurements Obtained from the Three-dimensional Printing Model of the MV in Controls and in Patients with RMVD and DMVD

	Controls (n = 15)	RMVD (n = 15)	DMVD (n = 15)
Annulus			
AP (cm)	2.89 ± 0.30	3.34 ± 0.43[a]	3.52 ± 0.71[a]
AL-PM (cm)	3.29 ± 0.31	3.45 ± 0.60	3.98 ± 0.34[a]
CW (cm)	3.23 ± 0.41	3.42 ± 0.54	3.88 ± 0.21[a]
AC (cm)	10.66 ± 0.82	11.10 ± 0.80	12.15 ± 1.61[ab]
A (cm^2)	8.05 ± 1.60	10.30 ± 1.30	11.72 ± 3.10[a]
AH (cm)	0.73 ± 0.19	0.70 ± 0.15	0.58 ± 0.17[a]
AHCWR (%)	23.00 ± 6.00	21.00 ± 5.00	15.00 ± 4.00[ab]
Leaflets (mm^2)			
AL (cm)	2.21 ± 0.37	2.66 ± 0.28[a]	2.38 ± 0.45[ab]
PL (cm)	1.21 ± 0.30	1.44 ± 0.23	1.42 ± 0.52[a]
AA (cm^2)	5.44 ± 1.89	6.77 ± 1.19[a]	6.27 ± 1.74 [a]
PA (cm^2)	4.05 ± 0.95	4.94 ± 2.03	5.69 ± 2.71 [a]

Data are expressed as mean ± standard deviation. [a]$P < 0.05$ versus control subjects. [b]$P < 0.05$ versus RMVD.
A, annular area; AA, anterior leaflet area; AC, annular circumference; AH, annular height; AHCWR, annular height to commissural width ratio; AL, length of anterior leaflet; AL-PM, anterolateral and posteromedial diameters; AP, anteroposterior diameters; CW, commissural width; DMVD, degenerative mitral valve disease; PA, area of posterior leaflet; PL, length of posterior leaflet; RMVD, rheumatic mitral valve disease.

The geometric parameter of the mitral valve is presented in **Table 5**.

Compared with the control group, patients of the RMVD group had larger AL and AA ($P < 0.05$); the AP, ALPM, CW, AH, AHCWR, AC, A, PL, and PA were not significantly different from those of the normal group ($P > 0.05$). These measurements demonstrated that the annulus was not significantly expanded or flat, and the anterior leaflet became lengthier and larger. The 3D printing model can reflect the thickened and fused leaflets and granular calcification (**Figure 4**).

Patients of the DMVD group had dilated mitral annulus with significantly increased AP, ALPM, CW, AC, and A ($P < 0.05$), and the reduction in AH and AHCWR ($P < 0.05$) represented the flattening of the mitral annulus. The length and area of anterior and posterior leaflets increased significantly in the DMVD groups ($P < 0.05$). The 3D printing model demonstrated that the annulus diameter was significantly larger than that of the RMVD group, and it showed the location and extent of the prolapsed leaflet (**Figure 5**).

Mitral repair simulations on the 3D printing model

Two experienced surgeons performed MV repair on 10 models (**Figure 6**; **Table 6**). The increases in CL and AHCWR in the models were similar those of the actual patient mitral repair (**Table 7**). Bland-Altman plots demonstrated good agreement between these two parameters in the simulated operations on the 3D printing model and the actual surgery on the patient valve (**Figure 7**). The strongest correlation with the degree of MR was observed with CL (r = –0.87, $P < 0.01$; **Figure 8A**). The higher degree of MR was also related to lower AHCWR (r = –0.79, $P < 0.01$; **Figure 8B**).

The model of patient C underwent two different repair strategies to evaluate the effects of the two strategies and choose superior surgical planning. Patient C had posterior leaflet and commissural prolapse and underwent repair by prolapse leaflet rectangle resection and ring annuloplasty and by posterior leaflet triangular resection, commissure closure, and ring annuloplasty. Both mitral repair strategies resulted in increasing leaflet coaptation; however, the latter had a superior effect on increasing the coaptation length and restoring the shape of the annulus as opposed to the former (CL, 0.85 versus 0.96 cm; AHCWR, 18.9% versus 20.5%).

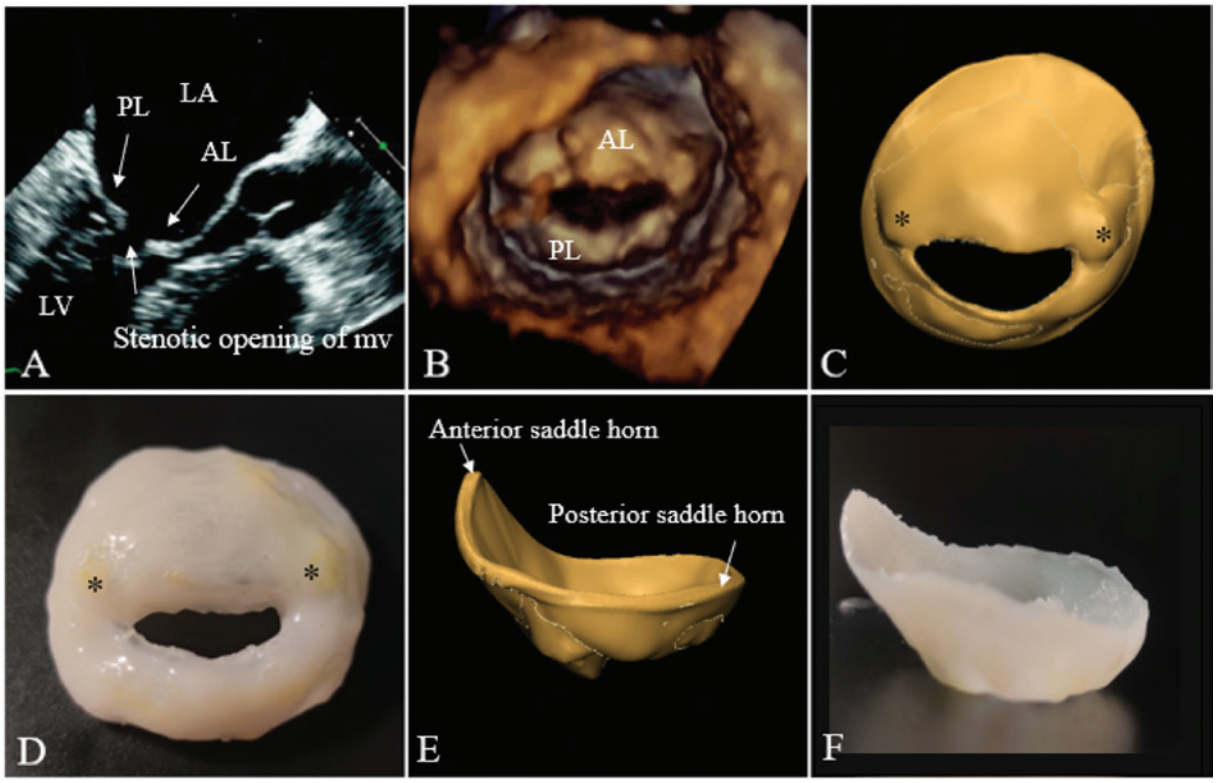

Figure 4 2D and 3D TEE images and virtual and silicone valve models of a patient with RMVD. (A) Long-axis view of the left ventricle and atrium during diastole. The relative positions of the AL and PL are indicated. (B) 3D TEE model. Virtual (C) and silicone (D) models viewed from the left ventricle, the stenotic opening of mitral valve, thickened valves, and yellow granular calcification (*) can be reflected. Virtual (E) and silicone (F) models as viewed in profile from the anterior to the posterior commissures. 2D, two-dimensional; 3D, three-dimensional; AL, anterior mitral valve leaflet; PL, posterior mitral valve leaflet; RMVD, rheumatic mitral valve disease; TEE, transesophageal echocardiography.

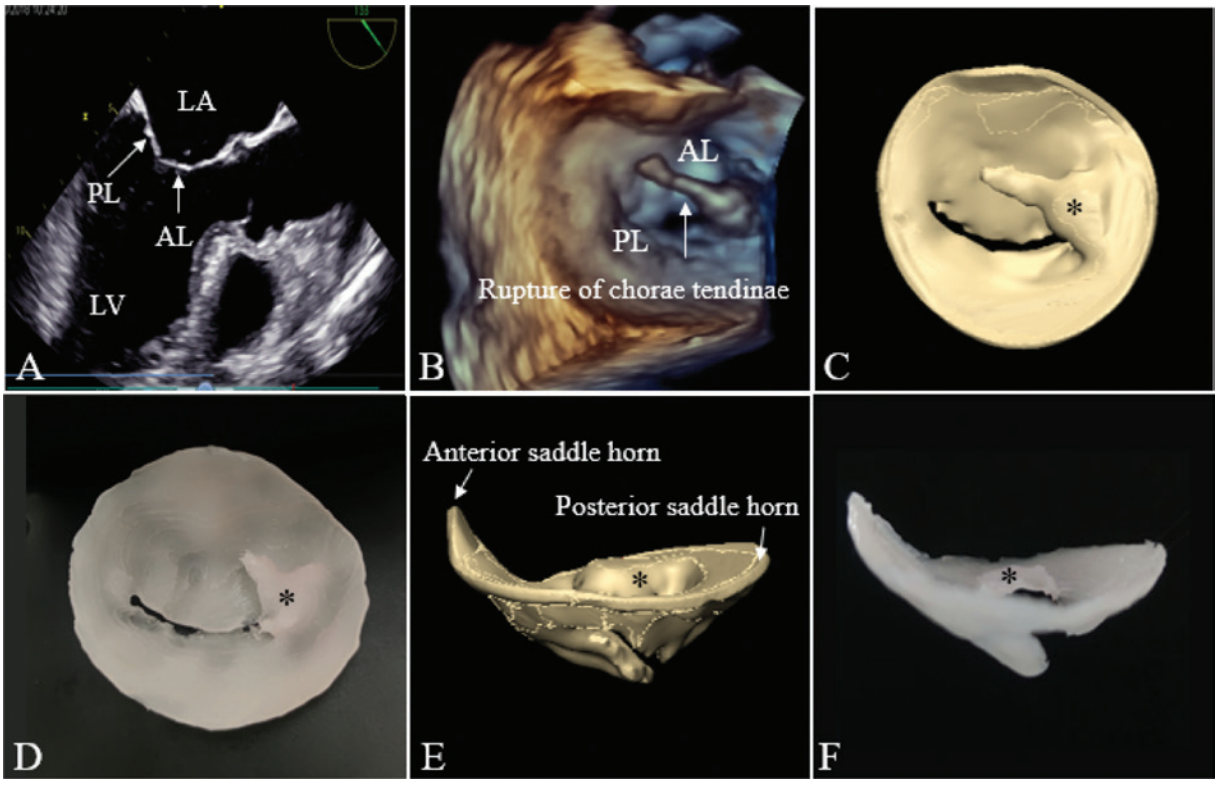

Figure 5 2D and 3D on TEE images and virtual and silicone valve models of a patient with P3 leaflet prolapse. (A) Long-axis view of the left ventricle and atrium during systole. The relative positions of the AL and PL are indicated. (B) 3D TEE model. Virtual (C) and silicone (D) models viewed from the left atrium; P3 leaflet prolapse (*) and rupture of chordae tendineae can be seen. Virtual (E) and silicone (F) models as viewed in profile from the anterior to the posterior commissures, in which the flat annulus can be appreciated (versus **Figure 4E, F**). 2D, two-dimensional; 3D, three-dimensional; AL, anterior mitral valve leaflet; PL, posterior mitral valve leaflet; TEE, transesophageal echocardiography.

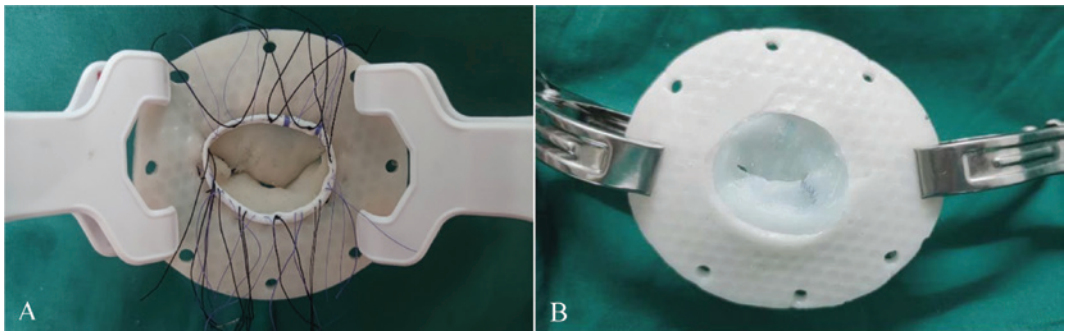

Figure 6 Variety of repairs performed on models: (A) annuloplasty ring being parachuted down onto the model and (B) suturing the posterior leaflet of a model during a triangular tissue resection repair.

Table 6 Mitral Repair Completed on Model and Patient Valves

Surgical Plan	Model Valve (n = 10)	Patient Valve (n = 10)
Triangular resection	3 (30)	4 (40)
Rectangle resection	3 (30)	2 (20)
Commissure closure	1 (10)	2 (20)
Edge-to-edge repair	1 (10)	1 (10)
Folding repair	2 (20)	2 (20)
Annuloplasty ring	10 (100)	10 (100)

Data are expressed as number (percentage).

Discussion

In our experiments, the principal results are as follows: the 3D printing model could intuitively display the morphological characteristics of the rheumatic and degenerative mitral disease and provide quantitative anatomical information for the clinic; (2) the silicone 3D printing model could be applied to mitral repair simulation, providing decision-making information for the clinic based on morphological changes after surgery.

We observed morphological characteristics of rheumatic and degenerative mitral disease based on the 3D printing model. Both the RMVD and DMVD groups showed significant differences in the MV structure compared with the normal group. In the RMVD group, the difference mainly lay in the leaflets, with the AL and AA increasing. Adhesion at the junction, calcification, and thickening on leaflets as well as chordae fusion shortening restricted the leaflets' opening and the annulus' movement or expansion [9]. Meanwhile, in the DMVD group, the AP, ALPM, CW, AC, and A increased, and parameters of AH and AHCWR reduced obviously, indicating that the original "saddle" shape of the MV annulus became flat and dilated. Previous studies have found that AHCWR can reflect the 3D degree of the annulus, and a smaller value indicates that the annulus becomes flat [10], and the group of DMVD had increased leaflet area of anterior as well as posterior.

Although many methods for quantitative assessment of MV anatomy exist [11], the 3D printing model of the MV not only could quantitatively evaluate the morphological characteristics of the annulus and leaflets but could also intuitively display the pathology structure of the annulus and leaflets, which were the most important basis for choosing between MV repair and replacement [12]. Mitral repair remains the standard treatment for severe mitral regurgitation with better survival rates, better preservation of the left ventricle function, and lower complications [13, 14]. However, mitral repair involves many procedures, which are becoming more

Table 7 Measurements of the Patient and Model Valves Before and After Mitral Valve Repair

Patient	Model Valve				Patient Valve					
	Coaptation Length (cm)		AHCWR (%)		Coaptation Length (cm)		AHCWR (%)		Regurgitation Grade	
	Pre	Post	Pre	Post	Pre	Post	Pre	Post	Pre	Post
A	0.49	0.84	19.60	23.40	0.53	0.88	19.20	23.60	3	1
B	0.51	0.89	15.60	21.20	0.55	0.94	16.30	21.60	3	1
C	0.45	0.96	14.90	20.50	0.44	0.87	14.30	20.90	4	1
D	0.45	0.87	15.50	20.50	0.43	0.90	15.30	20.80	4	1
E	0.40	0.78	11.50	20.90	0.47	0.80	11.30	20.50	4	2
F	0.47	0.95	18.40	24.50	0.50	0.91	19.80	24.80	3	1
G	0.48	0.83	16.20	22.40	0.51	0.85	17.30	22.90	3	1
H	0.39	0.76	12.40	20.40	0.42	0.78	12.90	20.30	4	2
I	0.42	0.85	13.60	20.10	0.46	0.86	14.80	20.40	4	2
J	0.43	0.88	14.30	20.30	0.48	0.89	15.30	20.90	4	1
Mean ± standard deviation	0.45 ± 0.04	0.86 ± 0.06	15.20 ± 2.49	21.42 ± 1.51	0.48 ± 0.04	0.87 ± 0.05	15.65 ± 2.63	21.67 ± 1.56	3.60 ± 0.52	1.30 ± 0.48
P	<0.05		<0.05		<0.05		<0.05		<0.05	

AHCWR, annular height to commissural width ratio; pre, pre-repair; post, post-repair.

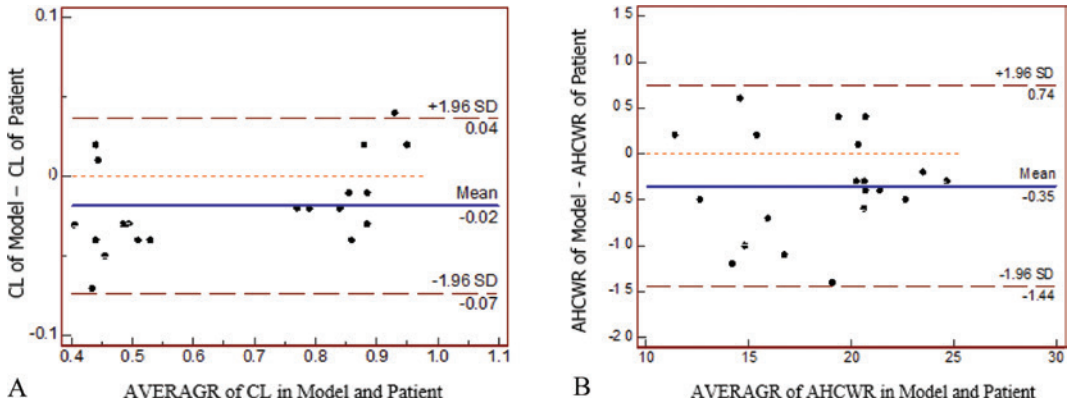

Figure 7 Bland-Altman plots showing agreement in the measurements obtained in the simulated operations on three-dimensional printing model and the actual surgery on patient valve. (A) Length of the coaptation. (B) Ratio of the annular height to the commissural width (AHCWR).

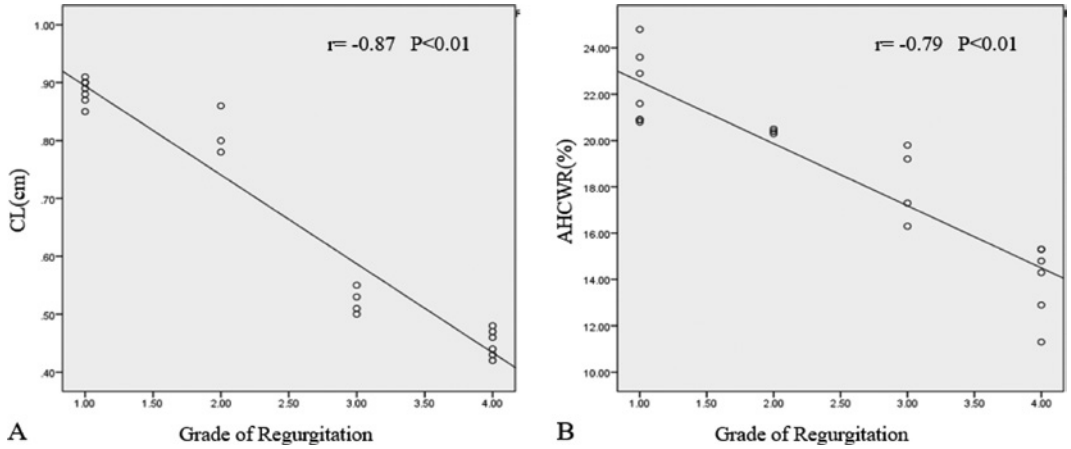

Figure 8 Correlations of regurgitation grade with coaptation length and annular height to commissural width ratio (AHCWR). The scatterplot demonstrates an inverse correlation between regurgitation grade and coaptation length (A) and an inverse correlation between regurgitation grade and AHCWR (B).

refined, individualized, and localized, and the MV's reparability depends on patient anatomy and surgeon experience [15]. Therefore, the more important advantage of the 3D printing model was that it could provide preoperative simulation, assist in the surgical decision-making, and improve the success rate of surgery, which cannot be provided by quantitative software evaluation.

To simulate mitral repair before the actual operation, our research used silicone as material, which was most suitable for simulating the material properties of the valve [16], but the silicone could not be used in the 3D printer directly. Therefore, the silicone valve models were generated by creating molds printed with water-soluble polyvinyl alcohol, then filled with RTV silicone. This method was widely used in 3D printing of valve and blood vessels and proved the superior material properties of silicone valve for simulation purposes [17].

In our research, we performed the mitral repair operation simulation on the model of 10 patients. The primary goal of mitral repair surgery was to increase leaflet coaptation and prevent further dilatation of the annulus [8]. A previous study has shown [7] that coaptation length and AHCWR were related to the degree of mitral regurgitation. Thus, our study evaluated the effect of mitral repair by comparing the measurement of the CL and AHCWR before and after repair. The simulated operation on the model was consistent with the measured value in the actual operation, indicating that the ability of the models to simulate mitral repair conditions and results similar to those experienced clinically by the patients. The correlation between the degree of MR with CL ($r = –0.87$, $P < 0.01$) and AHCWR ($r = –0.79$, $P < 0.01$) had also been confirmed in our research. More importantly, we could simulate multiple repair plans on the 3D printing model for some patients with complicated repairs and select the superiority of one strategy by morphological evaluation.

Limitations

There were several limitations in our study. The 3D printing model in our study mainly contained the structure of leaflets and annulus, whereas the chordae and papillary muscles were parallel to the ultrasound beam during imaging and could not be reconstructed well [18]. Therefore, the assessment and repair of the chordae and papillary muscle in MV disease was. Besides, the heart valves were a dynamic structure; the MV model we created was a static model and thus

cannot reflect the hemodynamic changes of the valve [19]. A study [20] assessed the 3D printing model dynamically combined with a phantom heart simulator. Moreover, the 3D printing model could reflect the morphological characteristics of RMVD, but the repair of RMVD was complicated. The patients in this study finally underwent MV replacement. Therefore, the application prospect of 3D printing models in RMVD requires us to explore further.

Conclusion

3D printing models of the MV from 3D TEE data could be used in the morphological analysis of the MV before and after surgery in DMVD, and these models could potentially assist in personalized mitral repair, in the evaluation the effectiveness of mitral repair based on morphological changes, and in improving the efficiency of complex mitral repairs and the ability of inexperienced surgeons.

Conflict of interest

All authors have no conflict of interest to declare.

Funding

This study was supported by a grant from the National Natural Science Foundation of China (grant no. 81771849).

References

[1] Krawczyk-Ożóg A, Hołda MK, Sorysz D, Koziej M, Siudak Z, et al. Morphologic variability of the mitral valve leaflets. J Thorac Cardiovasc Surg 2017;154:1927-35. [PMID: 28893395 DOI: 10.1016/j.jtcvs.2017.07.067]

[2] Iung B, Vahanian A. Epidemiology of acquired valvular heart disease. Can J Cardiol 2014;30:962-70. [PMID: 24986049 DOI: 10.1016/j.cjca.2014.03.022]

[3] Garbi M, Monaghan MJ. Quantitative mitral valve anatomy and pathology. Echo Res Pract 2015;2:R63-72. [PMID: 26693344 DOI: 10.1530/ERP-15-0008]

[4] Vahanian A, Alfieri O, Andreotti F, Antunes MJ, Baumgartner H, et al. Guidelines on the management of valvular heart disease (Version 2012). Eur Heart J 2012;33:2451-96. [PMID: 22922415 DOI: 10.1093/eurheartj/ehs109]

[5] Farooqi KM, Sengupta PP. Echocardiography and three-dimensional printing: sound ideas to touch a heart. J Am Soc Echocardiogr 2015;28:398-403. [PMID: 25839152 DOI: 10.1016/j.echo.2015.02.005]

[6] Maffessanti F, Marsan NA, Tamborini G, Sugeng L, Caiani EG, et al. Quantitative analysis of mitral valve apparatus in mitral valve prolapse before and after annuloplasty: a three-dimensional intraoperative transesophageal study. J Am Soc Echocardiogr 2011;24:405-13. [PMID: 21353470 DOI: 10.1016/j.echo.2011.01.012]

[7] Lee APW, Hsiung MC, Salgo IS, Fang F, Xie JM, et al. Quantitative analysis of mitral valve morphology in mitral valve prolapse with real-time 3-dimensional echocardiography: importance of annular saddle shape in the pathogenesis of mitral regurgitation. Circulation 2013;127:832-41. [PMID: 23266859 DOI: 10.1161/CIRCULATIONAHA.112.118083]

[8] Maisanoa F, Falk V, Borger MA, Vanermen H, Alfieri O, et al. Improving mitral valve coaptation with adjustable rings: outcomes from a European multicentre feasibility study with a new-generation adjustable annuloplasty ring system. Eur J Cardiothorac Surg 2013;44:913-8. [PMID: 23530026 DOI: 10.1093/ejcts/ezt128]

[9] Marijon E, Mirabel M, Celermajer DS, Jouven X. Rheumatic heart disease. Lancet 2012;379:953-64. [PMID: 22405798 DOI: 10.1016/S0140-6736(11)61171-9]

[10] Nguyen TC, Itoh A, Carlhäll CJ, Bothe W, Timek TA, et al. The effect of pure mitral regurgitation on mitral annular geometry and three-dimensional saddle shape. J Thorac Cardiovasc Surg 2008;136:557-65. [PMID: 18805251 DOI: 10.1016/j.jtcvs.2007.12.087]

[11] Shanks M, Delgado V, Ng ACT, van der Kley F, Schuijf JD, et al. Mitral valve morphology assessment three-dimensional transesophageal echocardiography versus computed tomography. Ann Thorac Surg 2010;90:1922-9. [PMID: 21095337 DOI: 10.1016/j.athoracsur.2010.06.116]

[12] Madesis A, Tsakiridis K, Zarogoulidis P, Katsikogiannis N, Machairiotis N, et al. Review of mitral valve insufficiency: repair or replacement. J Thorac Dis 2014;6:S39-51. [PMID: 24672698 DOI: 10.3978/j.issn.2072-1439.2013.10.20]

[13] Althunayyan A, Petersen SE, Lloyd G, Bhattacharyya S. Mitral valve prolapse. Expert Rev Cardiovasc Ther 2019;17:43-51. [PMID: 30484338 DOI: 10.1080/14779072.2019.1553619]

[14] Coutinho GF, Correia PM, Branco C, Antunes MJ. Long-term results of mitral valve surgery for degenerative anterior leaflet or bileaflet prolapse: analysis of negative factors for repair, early and late failures, and survival. Eur J Cardiothorac Surg 2016;50:66-74. [PMID: 26792923 DOI: 10.1093/ejcts/ezv470]

[15] Adams DH, Rosenhek R, Falk V. Degenerative mitral valve regurgitation: best practice revolution. Eur Heart J 2010;31:1958-66. [PMID: 20624767 DOI: 10.1093/eurheartj/ehq222]

[16] Ginty O, Moore J, Peters T, Bainbridge D. Modeling patient-specific deformable mitral valves. J Cardiothorac Vasc Anesth 2018;32:1368-73. [PMID: 29221976 DOI: 10.1053/j.jvca.2017.09.005]

[17] Scanlan AB, Nguyen AV, Ilina A, Lasso A, Cripe L. Comparison of 3D echocardiogram-derived 3D printed valve models to molded models for simulated repair of pediatric atrioventricular valves. Pediat Cardiol 2018;39:538-47. [PMID: 29181795 DOI: 10.1007/s00246-017-1785-4]

[18] Vukicevic M, Puperi DS, Jane Grande-Allen K, Little SH. 3D printed modeling of the mitral valve for catheter-based structural interventions. Ann Biomed Eng 2017;45:508-19. [PMID: 27324801 DOI: 10.1007/s10439-016-1676-5]

[19] Jiang L, Owais K, Matyal R, Khabbaz KR, Liu DC, et al. Dynamism of the mitral annulus: a spatial and temporal analysis. J Cardiothorac Vasc Anesth 2014;28:1191-7. [PMID: 25130425 DOI: 10.1053/j.jvca.2014.03.020]

[20] Ginty OK, Moore JM, Xu Y, Xia W, Fujii S, et al. Dynamic patient-specific three-dimensional simulation of mitral repair: can we practice mitral repair preoperatively? Innovations (Phila) 2018;13:11-22. [PMID: 29470257 DOI: 10.1097/IMI.0000000000000463]